

## **CHAPTER III**

### **RANDOM FIELD REPRESENTATION OF HORIZONTAL DENSITY DISTRIBUTION IN PARTIALLY ORIENTED FLAKEBOARD MAT**

#### **Abstract**

A random field representation of the horizontal density distribution in partially oriented flakeboard mats was investigated. The orientation of flakes can be characterized by both the Von Mises distribution and the uniform distribution within a range of angles. Theoretical models of the correlation coefficients of any two points simultaneously covered by one flake, variance functions of local density, characteristic area of the correlation, and the degree of orientation were developed. Results indicate that the concentration factor  $k = 700$  is sufficiently large to represent a perfectly aligned flake arrangement in oriented flakeboards based on the Von Mises distribution. The correlation coefficients of two points in a mat have a lower bound (random case) and an upper bound (perfectly aligned) in both Von Mises and uniform distributions. The variance is considerably reduced when the sampling zone size is within the length of flake. Based on the concept of characteristic area, where the minimum characteristic area is the area of a flake and the maximum characteristic area is approximate to the square of flake length, the degree of orientation in a panel can be represented as a function of characteristic area. This value is found to be very close to the percent alignment definition.

### **3.1. Introduction**

Oriented strand boards (OSB) are made by processing relatively low value and under-utilized wood materials into strands or flakes, which are approximately 100 mm in length, 15-20 mm in width and roughly 0.6-0.8 mm in thickness. After the flakes are dried, adhesives and wax are applied, and the flakes are typically formed into a three-layer mat. The top and bottom (face) layers are partially oriented along the long axis of the panel to provide added bending strength and stiffness in the direction of orientation while flakes in the middle (core) layer of the mat are randomly oriented. The mat is bonded together under heat and pressure to produce panels of various dimensions and thicknesses. OSB panels are very versatile as their mechanical and physical properties can be controlled by adjustment of production parameters to meet end users' demands for such characteristics as size, density and strength.

The various production parameters that influence OSB performance include species, flake geometry, flake lay up / orientation process (flakeboard structure), adhesive type and distribution mechanism, and pressing process. Many researchers have shown great interest in flakeboard structures and properties (Dai and Steiner 1994, Lang and Wolcott 1996, Suchsland and Xu 1989, Triche and Hunt 1993, Xu and Steiner 1995). In particular, Dai and Steiner (1994) studied the spatial correlation of flake coverage by making use of the theories in random fibrous network (Dodson 1971) to define the horizontal density distribution in panels with completely random flake orientation and position. The statistics of the horizontal density distribution in OSB are of particular interest in the assessment of product quality and performance. While most of the research has focused on completely random orientation of flakes and its influences on physical and mechanical strength properties of the panels, the

flake orientation in both face layers of OSB is in reality, partially random. There has been no theoretical consideration of the relationship between partially random orientation of flakeboards with physical properties such as the variation of board density and degree of orientation in the horizontal direction in the OSB products.

Since two orientation angles  $\mathbf{q}$  and  $\mathbf{q} + n\mathbf{p}$  ( $n = 1,2,3,\dots$ ) cannot be distinguished for a rectangular flake placed in a mat, the range of angles from  $-\frac{\mathbf{p}}{2}$  to  $+\frac{\mathbf{p}}{2}$  radian can completely describe all possible choices for flake orientation. The random distribution of flake orientation within a mat is an excellent example of axial data, which can be best described by the Von Mises distribution (Mardia 1972). Harris and Johnson (1982) pointed out that the concentration parameter of the Von Mises distribution ( $k$ ) can be used to characterize the distribution of flake orientations in flakeboards. Shaler (1991) compared two measures of flake alignment based on the Von Mises distribution of flake alignment and the classical definition of percent alignment given by Geimer (1976), which in fact is a linear transformation of the first moment (arithmetic mean) of the absolute value of angles in the range of  $\pm\frac{\mathbf{p}}{2}$  radian. Computer simulations yielded good agreement with theoretical calculations (Shaler 1991). Lau (1981) linked the standard deviation of normal distribution with the range of orientation angles by a factor of  $\sqrt{\frac{\mathbf{p}}{2}}$ .

This section presents a theoretical model of the horizontal density distribution of partially oriented flakeboard mat. The objectives of this study are:

- 1) to develop a random field representation of horizontal density distribution for partially oriented flakeboards following the Von Mises distribution and the uniform distribution,

- 2) to introduce the concept of characteristic area as a measure of within member correlation of horizontal density distribution, and
- 3) to characterize the degree of orientation as compared with the traditional definition of percent alignment (Geimer 1976).

### 3.2. Theoretical Model

#### 3.2.1. Probability density function for flake orientation

Due to the forming process of OSB, the orientation of the principal direction of each flake is partially random. Mardia (1972) provided a comprehensive description of the statistics of directional data. One of the most important properties of such a random variable  $\mathbf{q}$  (in radian) is that its probability density function  $f(\mathbf{q})$  has a circular form:

$$f(\mathbf{q} \pm n\mathbf{p}) = f(\mathbf{q}) \quad \left(-\frac{\mathbf{p}}{2} \leq \mathbf{q} \leq \frac{\mathbf{p}}{2}\right) \quad (n = 1, 2, 3, \dots) \quad (3.1)$$

since a flake oriented at  $\mathbf{q}$  to the  $x$  direction is the same as a flake oriented at  $\mathbf{q} \pm n\mathbf{p}$ . A function for characterizing directional axial data is the Von Mises probability density function (PDF) whose axial functional form is given: (Harris and Johnson 1982):

$$f(\mathbf{q}, \mathbf{q}_1, k) = \begin{cases} \frac{1}{2\mathbf{q}_1 I_0(k)} e^{k \cos[2(\mathbf{q} - \mathbf{q}_0)]} & (-\mathbf{q}_1 \leq \mathbf{q} \leq \mathbf{q}_1, \text{ and } 0 < \mathbf{q}_1 \leq \frac{\mathbf{p}}{2}) \\ 0 & \text{otherwise} \end{cases} \quad (3.2)$$

where  $k$  is the concentration parameter to specify the shape of the distribution,

$q_0$  is the mean value of the orientation angles,

$q_1$  equals to  $\frac{\mu}{2}$  when  $k > 0$ , which means that the range of flake orientation angles in

the Von Mises distribution must be between  $-\frac{\mu}{2}$  and  $\frac{\mu}{2}$ , and

$I_0(k)$  is the modified Bessel function of the first kind, order zero.

$$I_n(k) = \sum_{m=0}^{\infty} \frac{\left(\frac{k}{2}\right)^{2m+n}}{(m+n)!m!} \quad (3.3)$$

Another property of this PDF is that the integration of the PDF over the range of  $-\frac{\mu}{2} \leq q \leq \frac{\mu}{2}$  equals to one, *i.e.*,

$$\int_{-q_1}^{q_1} f(q, q_1, k) dq = \frac{1}{2q_1 I_0(k)} \int_{-q_1}^{q_1} e^{k \cos[2(q-q_0)]} dq = 1 \quad (3.4)$$

Based on **Equation 3.4**, a PDF without the Bessel function can be obtained from **Equation 3.2** as:

$$f(q, q_1, k) = \frac{e^{k \cos[2(q-q_0)]}}{\int_{-q_1}^{q_1} e^{k \cos[2(j-q_0)]} dj} \quad (3.5)$$

When  $k \rightarrow 0$ ,  $f(q, q_1, 0) = \frac{1}{2q_1}$ , which represents a uniform distribution of orientation angles.

When  $k \rightarrow \infty$ , the distribution reduces to a point distribution, which can be described by the Dirac delta function (the perfectly aligned case).

### 3.2.2. Point-to-point variance of the density

Let  $D(x, y)$  represents the point-to-point horizontal density profile in the  $x$ - $y$  plane in a mat. The variation of the point-to-point density in the two-dimensional random flake network was obtained from Dai and Steiner (1994):

$$\text{var}(D) = \frac{\mathbf{t}_f \mathbf{r}_f \mathbf{r}}{\mathbf{t}} \quad (3.6)$$

where  $\mathbf{t}_f$  is the flake thickness,  $\mathbf{r}_f$  is the flake density,  $\mathbf{t}$  is the thickness of the mat, and  $\mathbf{r}$  is the mean density of the mat.

Consider dividing the two-dimensional domain into a large number of small, non-overlapping, congruent, rectangular, sampling zones,  $A(x, y)$ , with side length  $S_x$  and width  $S_y$ , where  $x, y$  represents the coordinates of the centroid of a sampling zone. The local average of density is given by integrating the density profile  $D(x, y)$  over the rectangular area of  $A$  (Vanmarcke 1983):

$$D_A(x, y) = \frac{1}{S_x S_y} \int_{x-\frac{S_x}{2}}^{x+\frac{S_x}{2}} \int_{y-\frac{S_y}{2}}^{y+\frac{S_y}{2}} D(x, y) dx dy \quad (3.7)$$

The information about point-to-point variation is contained in the variance function, as the variance between values of the random field at two locations. The variance of density between the regions,  $\text{var}(D_A)$ , can be expressed as (Vanmarcke 1983):

$$\text{var}(D_A) = \mathbf{g}(x, y) \text{var}(D) \quad (3.8)$$

where  $\mathbf{g}(x, y)$  is defined as the variance function of the density. It can be noted that  $\mathbf{g}(x, y)$  has

the limiting value of one as the sampling zone reduces to a point and zero as the zone size approaches infinity.

### 3.2.3. Variance function of the density

The variance function,  $g(x,y)$ , in a two-dimensional domain is defined as the ratio of the variance of the local average,  $D_A(x, y)$ , over a rectangular area  $A (= S_x \times S_y)$  and the "point" variance of the original process,  $D(x, y)$ . The variance function is related to the correlation function ( $\mathbf{a}$ ) and the probability density function ( $\mathbf{b}$ ) for two points within a rectangle as (Dodson 1971),

$$g(S_x, S_y, \mathbf{l}, \mathbf{w}, \mathbf{q}_1, k) = \int_0^{r_{max}} \mathbf{b}(S_x, S_y, r) \cdot \mathbf{a}(\mathbf{l}, \mathbf{w}, \mathbf{q}_1, k, r) dr \quad (3.9)$$

where  $r_{max}$  is a random variable depending on the flake geometry ( $\mathbf{l}, \mathbf{w}$ ) and the sampling zone size ( $S_x, S_y$ );  $\mathbf{q}_1$  is another random variable in the uniform distribution ( $k = 0$ ), and  $\mathbf{q}_1 = \frac{\mu}{2}$  in the Von Mises distribution ( $k \neq 0$ ).

### 3.2.4. Correlation coefficient for two points in a rectangle

Consider the distribution of two-dimensional flakes with length  $\mathbf{l}$  and width  $\mathbf{w}(\mathbf{w} \leq \mathbf{l})$ , it is assumed that the long axes of these flakes are oriented at an angle of  $\mathbf{q} + d\mathbf{q}$  from a given reference direction, usually  $x$  direction. The random location of the flake centroids are assumed to follow a Poisson distribution (Dai and Steiner 1994) of overlap intensity  $d\mathbf{m}(\mathbf{q})$  per unit area. Therefore, the superposition of such processes, for  $-\frac{\mu}{2} < \mathbf{q} \leq \frac{\mu}{2}$ , produces a distribution of overlaps with intensity  $\mathbf{m}$  per unit area for the total number of flake centres as:

$$d\mathbf{m}(\mathbf{q}, \mathbf{q}_1, k) = \mathbf{m}f(\mathbf{q}, \mathbf{q}_1, k)d\mathbf{q} = \frac{\mathbf{m}e^{k \cos[2(\mathbf{q}-\mathbf{q}_0)]}}{\int_{-\mathbf{q}_1}^{\mathbf{q}_1} e^{k \cos[2(j-\mathbf{q}_0)]} d\mathbf{j}} d\mathbf{q} \quad (3.10)$$

Correlation coefficient,  $\mathbf{a}$ , between the number of flake overlaps at two points,  $p$  and  $q$  separated by a distance of  $r$  is given as (Dodson 1971)

$$\mathbf{a}(\mathbf{l}, \mathbf{w}, \mathbf{q}_1, k, r) = \frac{\text{var}(N_{pq})}{\text{var}(N_p)} \quad (3.11)$$

where  $N_{pq}$  is the number of flakes that cover both  $p$  and  $q$ , and  $N_p$  is the total number of flakes that cover only  $p$ . It therefore follows that both  $N_{pq}$  and  $N_p$  are Poisson distributed with the variances equal to

$$\text{var}(N_p) = \int_{-\mathbf{q}_1}^{\mathbf{q}_1} \mathbf{l} \mathbf{w} d\mathbf{m}(\mathbf{q}) = \mathbf{l} \mathbf{w} \mathbf{m} \quad (3.12)$$

$$\text{var}(N_{pq}) = \int_{-\mathbf{q}_1}^{\mathbf{q}_1} (\mathbf{w} - r \sin|\mathbf{q}|)(\mathbf{l} - r \cos\mathbf{q}) d\mathbf{m}(\mathbf{q}) \quad (3.13)$$

where  $(\mathbf{w} - r \sin|\mathbf{q}|)(\mathbf{l} - r \cos\mathbf{q})$  is the total area containing the centres of flakes that cover both  $p$  and  $q$ .

Applying  $d\mathbf{m}(\mathbf{q})$  from **Equation 3.10** into **Equation 3.13** and combining **Equations 3.11** to 3.13, it can be shown that the correlation coefficient,  $\mathbf{a}$ , is:

$$\mathbf{a}(\mathbf{l}, \mathbf{w}, \mathbf{q}_1, k, r) = \frac{\text{var}(N_{pq})}{\text{var}(N_p)} = \frac{\int_{-\mathbf{q}_1}^{\mathbf{q}_1} (1 - \frac{r}{\mathbf{w}} \sin|\mathbf{q}|)(1 - \frac{r}{\mathbf{l}} \cos\mathbf{q}) e^{k \cos[2(\mathbf{q}-\mathbf{q}_0)]} d\mathbf{q}}{\int_{-\mathbf{q}_1}^{\mathbf{q}_1} e^{k \cos[2(j-\mathbf{q}_0)]} d\mathbf{j}} \quad (3.14)$$

where  $r$  equals to the distance separated by two points  $p$  and  $q$ .

For all possible values of  $\mathbf{q}$  within the rectangular domain  $\mathbf{l} \times \mathbf{w}$ , using the symmetry properties of  $(\mathbf{w} - r \sin|\mathbf{q}|)(\mathbf{l} - r \cos \mathbf{q})$ , three ranges of angles are necessary to be taken into consideration where  $\Omega$  represents the integration intervals for  $\mathbf{q}$  at  $\mathbf{q}_1 = \frac{\mathbf{p}}{2}$  :

- 1)  $0 < r \leq \mathbf{w}$ , corresponding to  $\Omega = \{0 < \mathbf{q} \leq \frac{1}{2}\mathbf{p}\}$ ;
- 2)  $\mathbf{w} < r \leq \mathbf{l}$ , corresponding to  $\Omega = \{0 < \mathbf{q} \leq \arcsin(\frac{\mathbf{w}}{r})\}$ ;
- 3)  $\mathbf{l} < r \leq \sqrt{\mathbf{l}^2 + \mathbf{w}^2}$ , corresponding to  $\Omega = \{\arccos(\frac{\mathbf{l}}{r}) < \mathbf{q} \leq \arcsin(\frac{\mathbf{w}}{r})\}$ .

The correlation coefficient  $\mathbf{a}(\mathbf{l}, \mathbf{w}, \mathbf{q}_1, k, r)$  can be evaluated at arbitrary  $r$  and  $k$  ( $k \neq 0$ ). Of special interest is the limiting cases of  $k = 0$  and  $k = \infty$  which will be discussed in more detail as follows.

In cases where  $k = 0$  and  $\mathbf{q}_1 \leq \frac{\mathbf{p}}{2}$ , the Von Mises distribution becomes the uniform distribution with PDF of the following form:

$$f(\mathbf{q}, \mathbf{q}_1, 0) = \frac{1}{2\mathbf{q}_1} \quad (-\mathbf{q}_1 < \mathbf{q} \leq \mathbf{q}_1, \text{ and } 0 < \mathbf{q}_1 \leq \frac{\mathbf{p}}{2}) \quad (3.15)$$

Here  $\pm\mathbf{q}_1$  are the upper and lower bounds for orientation angle  $\mathbf{q}$ . It can take arbitrary values from 0 to  $\frac{\mathbf{p}}{2}$ . If  $\mathbf{q}_1$  approaches zero, all flakes are oriented parallel to each other; if  $\mathbf{q}_1$  equals to  $\frac{\mathbf{p}}{2}$ , it is completely randomized orientation. In the general case of partially random orientation,  $0 < \mathbf{q}_1 \leq \frac{\mathbf{p}}{2}$ , the exact form of the correlation coefficient is given for three ranges of  $\mathbf{q}_1$  (Figures 3.1a to 3.1c).

Range 1:  $\arcsin\left(\frac{\mathbf{w}}{\mathbf{l}}\right) < \mathbf{q}_1 \leq \frac{\mathbf{p}}{2}$

$$\mathbf{a}(\mathbf{l}, \mathbf{w}, \mathbf{q}_1, 0, r) = \begin{cases} 1 - \frac{1}{\mathbf{q}_1} \left[ \frac{r}{\mathbf{l}} \sin \mathbf{q}_1 - \frac{r}{\mathbf{w}} (\cos \mathbf{q}_1 - 1) - \frac{r^2}{2\mathbf{l}\mathbf{w}} \sin^2 \mathbf{q}_1 \right] & (0 < r \leq \frac{\mathbf{w}}{\sin \mathbf{q}_1}) \\ \frac{1}{\mathbf{q}_1} \left[ \arcsin\left(\frac{\mathbf{w}}{r}\right) - \frac{\mathbf{w}}{2\mathbf{l}} - \frac{r}{\mathbf{w}} + \frac{\sqrt{r^2 - \mathbf{w}^2}}{\mathbf{w}} \right] & (\frac{\mathbf{w}}{\sin \mathbf{q}_1} < r \leq \mathbf{l}) \\ \frac{1}{\mathbf{q}_1} \left[ \arcsin\left(\frac{\mathbf{w}}{r}\right) - \arccos\left(\frac{\mathbf{l}}{r}\right) - \frac{\mathbf{l}^2 + \mathbf{w}^2 + r^2}{2\mathbf{l}\mathbf{w}} + \frac{\sqrt{r^2 - \mathbf{w}^2}}{\mathbf{w}} + \frac{\sqrt{r^2 - \mathbf{l}^2}}{\mathbf{l}} \right] & (\mathbf{l} < r \leq \sqrt{\mathbf{l}^2 + \mathbf{w}^2}) \end{cases} \quad (3.16)$$

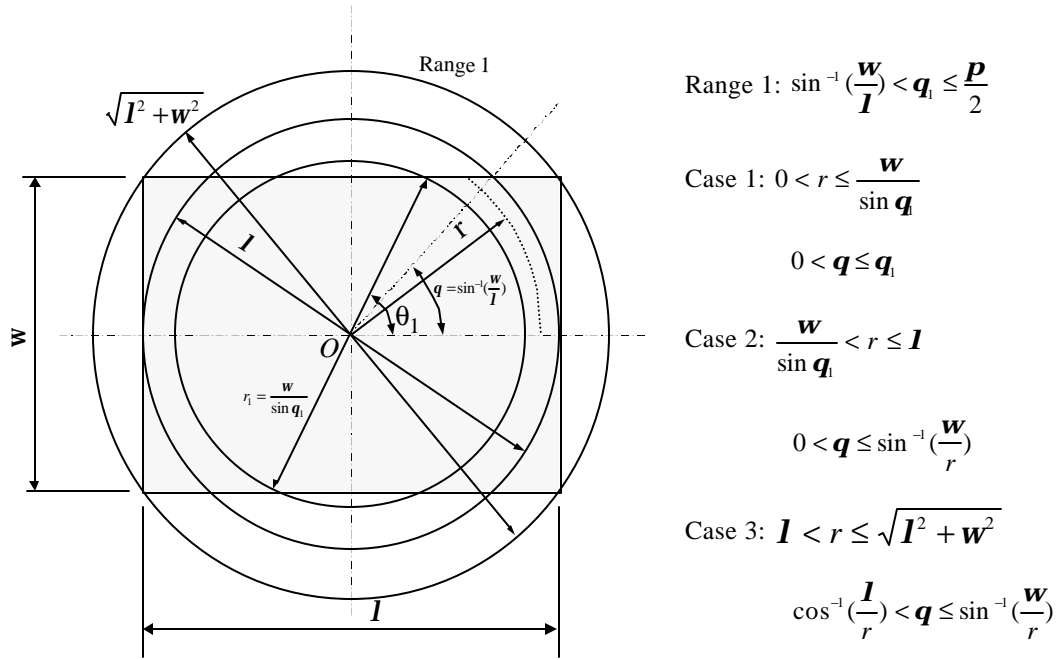
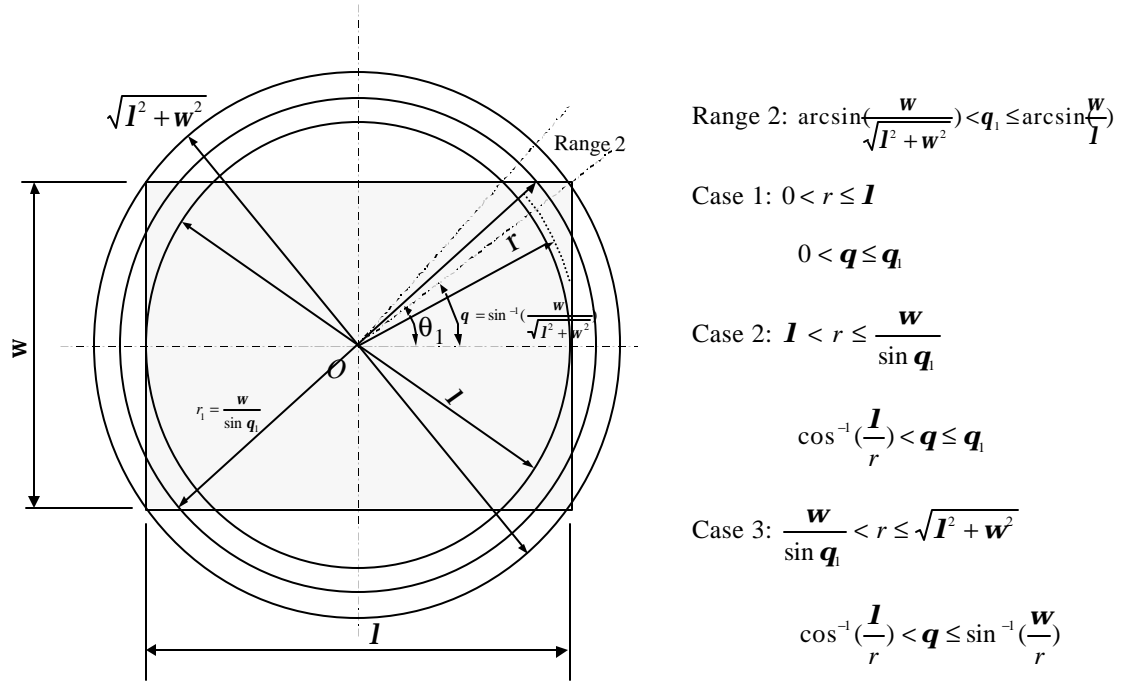


Figure 3.1a Schematic diagram for the range of angles within Range 1 for a flake with length  $\mathbf{l}$  and width  $\mathbf{w}$  during integration.

Range 2:  $\arcsin\left(\frac{w}{\sqrt{I^2 + w^2}}\right) < q_1 \leq \arcsin\left(\frac{w}{I}\right)$

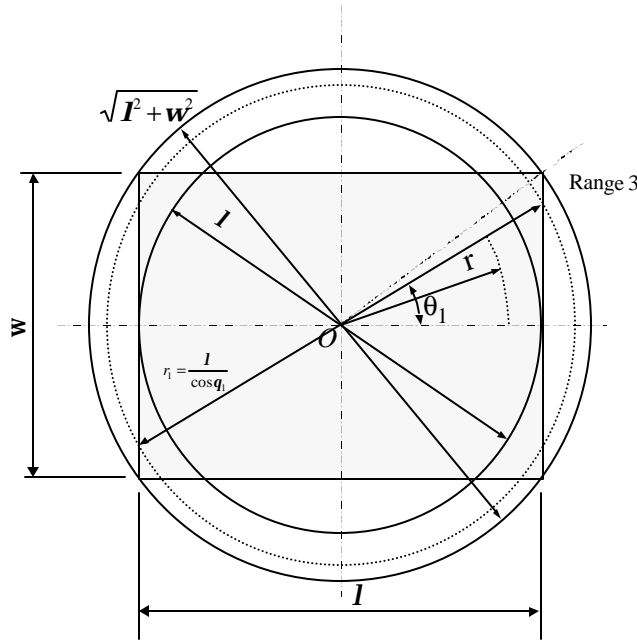
$$a(I, w, q_1, 0, r) = \begin{cases} 1 - \frac{1}{q_1} \left[ \frac{r}{I} \sin q_1 - \frac{r}{w} (\cos q_1 - 1) - \frac{r^2}{2Iw} \sin^2 q_1 \right] & (0 < r \leq I) \\ 1 - \frac{1}{q_1} \left[ \arccos\left(\frac{I}{r}\right) + \frac{r}{I} \sin q_1 - \frac{r}{w} \cos q_1 - \frac{r^2}{2Iw} \sin^2 q_1 + \frac{I^2 + r^2}{2Iw} - \frac{\sqrt{r^2 - I^2}}{I} \right] & (I < r \leq \frac{w}{\sin q_1}) \\ \frac{1}{q_1} \left[ \arcsin\left(\frac{w}{r}\right) - \arccos\left(\frac{I}{r}\right) - \frac{I^2 + w^2 + r^2}{2Iw} + \frac{\sqrt{r^2 - w^2}}{w} + \frac{\sqrt{r^2 - I^2}}{I} \right] & (\frac{w}{\sin q_1} < r \leq \sqrt{I^2 + w^2}) \end{cases} \quad (3.17)$$



**Figure 3.1b** Schematic diagram for the range of angles within Range 2 for a flake with length  $I$  and width  $w$  during integration.

Range 3:  $0 < \mathbf{q}_1 \leq \arcsin\left(\frac{\mathbf{w}}{\sqrt{\mathbf{I}^2 + \mathbf{w}^2}}\right)$

$$\mathbf{a}(\mathbf{I}, \mathbf{w}, \mathbf{q}_1, 0, r) = \begin{cases} 1 - \frac{1}{\mathbf{q}_1} \left[ \frac{r}{\mathbf{I}} \sin \mathbf{q}_1 - \frac{r}{\mathbf{w}} (\cos \mathbf{q}_1 - 1) - \frac{r^2}{2\mathbf{I}\mathbf{w}} \sin^2 \mathbf{q}_1 \right] & (0 < r \leq \mathbf{I}) \\ 1 - \frac{1}{\mathbf{q}_1} \left[ \arccos\left(\frac{\mathbf{I}}{r}\right) + \frac{r}{\mathbf{I}} \sin \mathbf{q}_1 - \frac{r}{\mathbf{w}} \cos \mathbf{q}_1 - \frac{r^2}{2\mathbf{I}\mathbf{w}} \sin^2 \mathbf{q}_1 + \frac{\mathbf{I}^2 + r^2}{2\mathbf{I}\mathbf{w}} - \frac{\sqrt{r^2 - \mathbf{I}^2}}{\mathbf{I}} \right] & (\mathbf{I} < r \leq \frac{\mathbf{I}}{\cos \mathbf{q}_1}) \end{cases} \quad (3.18)$$



Range 3:  $0 < \mathbf{q} \leq \arcsin\left(\frac{\mathbf{w}}{\sqrt{\mathbf{I}^2 + \mathbf{w}^2}}\right)$

Case 1:  $0 < r \leq \mathbf{I}$

$0 < \mathbf{q} \leq \mathbf{q}_1$

Case 2:  $\mathbf{I} < r \leq \frac{\mathbf{I}}{\cos \mathbf{q}_1}$

$\cos^{-1}\left(\frac{\mathbf{I}}{r}\right) < \mathbf{q} \leq \sin^{-1}\left(\frac{\mathbf{w}}{r}\right)$

**Figure 3.1c** Schematic diagram for the range of angles within Range 3 for a flake with length  $\mathbf{I}$  and width  $\mathbf{w}$  during integration.

When  $\mathbf{q}_1 = \frac{\pi}{2}$ , **Equation 3.16** represents the completely random case in the following form, which agrees with the finding of Dodson (1971):

$$\mathbf{a}(\mathbf{I}, \mathbf{w}, \frac{p}{2}, 0, r) = \begin{cases} 1 - \frac{2}{p} \left[ \frac{r}{\mathbf{I}} + \frac{r}{\mathbf{w}} - \frac{r^2}{2\mathbf{I}\mathbf{w}} \right] & (0 < r \leq \mathbf{w}) \\ \frac{2}{p} \left[ \arcsin\left(\frac{\mathbf{w}}{r}\right) - \frac{\mathbf{w}}{2\mathbf{I}} - \frac{r}{\mathbf{w}} + \frac{\sqrt{r^2 - \mathbf{w}^2}}{\mathbf{w}} \right] & (\mathbf{w} < r \leq \mathbf{I}) \\ \frac{2}{p} \left[ \arcsin\left(\frac{\mathbf{w}}{r}\right) - \arccos\left(\frac{\mathbf{I}}{r}\right) - \frac{\mathbf{I}^2 + \mathbf{w}^2 + r^2}{2\mathbf{I}\mathbf{w}} + \frac{\sqrt{r^2 - \mathbf{w}^2}}{\mathbf{w}} + \frac{\sqrt{r^2 - \mathbf{I}^2}}{\mathbf{I}} \right] & (\mathbf{I} < r \leq \sqrt{\mathbf{I}^2 + \mathbf{w}^2}) \end{cases} \quad (3.19)$$

If all flakes are perfectly aligned ( $\mathbf{q}_1 = 0$ ), the correlation coefficient is a function of flake length ( $\mathbf{I}$ ) and the distance ( $r$ ) between two arbitrarily chosen points on a line. When  $r = 0$ , the two points are common and the correlation coefficient equals unity. When the distance  $r$  between two points is greater than  $\mathbf{I}$ , the correlation coefficient is zero. It can be summarized as:

$$\mathbf{a}(\mathbf{I}, \mathbf{w}, 0, 0, r) = \begin{cases} 1 - \frac{r}{\mathbf{I}} & (0 \leq r \leq \mathbf{I}) \\ 0 & (r > \mathbf{I}) \end{cases} \quad (3.20)$$

**Equation 3.20** can also be obtained from **Equation 3.18** assuming  $\mathbf{q}_1 \rightarrow 0$ .

### 3.2.5. The probability density function for two points in a rectangle

The probability density function for the distance  $r$  between two points chosen independently and at random within a rectangle, of side length  $S_x$  and width  $S_y$  ( $S_x > S_y$ ), was given by Ghosh (1951) as:

$$\mathbf{b}(S_x, S_y, r) = \int_0^{\frac{p}{2}} \left[ \frac{4r}{S_x S_y} \left(1 - \frac{r}{S_y} \sin \mathbf{q}\right) \left(1 - \frac{r}{S_x} \cos \mathbf{q}\right) \right] d\mathbf{q} \quad (3.21)$$

Particularly, the integration results are as follows:

$$\mathbf{b}(S_x, S_y, r) = \begin{cases} \frac{4r}{S_x^2 S_y^2} \left[ \frac{\mathbf{p}}{2} S_x S_y - r(S_x + S_y) + \frac{r^2}{2} \right] & (0 \leq r \leq S_y) \\ \frac{4r}{S_x^2 S_y^2} \left[ S_x S_y \arcsin\left(\frac{S_y}{r}\right) - \frac{S_y^2}{2} + S_x \sqrt{r^2 - S_y^2} - S_x r \right] & (S_y \leq r \leq S_x) \\ \frac{4r}{S_x^2 S_y^2} \left[ S_x S_y \left[ \arcsin\left(\frac{S_y}{r}\right) - \arccos\left(\frac{S_x}{r}\right) \right] - \frac{S_x^2 + S_y^2 + r^2}{2} + S_x \sqrt{r^2 - S_y^2} + S_y \sqrt{r^2 - S_x^2} \right] & (S_x \leq r \leq \sqrt{S_x^2 + S_y^2}) \end{cases} \quad (3.22)$$

For square zones ( $S_x = S_y$ ), the central range ( $S_y \leq r \leq S_x$ ) for  $r$  is not required. Some typical distribution curves for the probability density in square zones are shown in **Figure 3.2**. It is noted that the distribution curves tend to flatten as the sampling zone size increases.

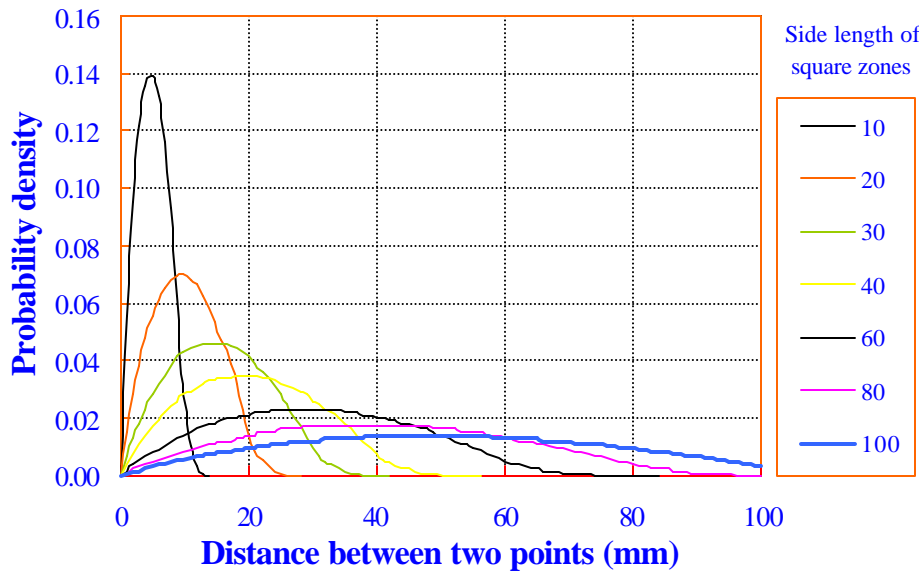


**Figure 3.2** Probability density for the distance between two points in square zones.

### 3.2.6. Characteristic area - a measure of correlation

In random field theory, the "characteristic area" is an important statistical parameter, which defines a measure of correlation in terms of the asymptotic form of the variance function in two dimensions. It can be expressed in terms of the variance and correlation functions.

When the sampling zone ( $S_x, S_y$ ) becomes relatively large, the variance function ( $g$ ) converges to an asymptotic expression. This property of variance function is defined by Vanmarcke (1983) as:

$$g(S_x, S_y, \mathbf{l}, \mathbf{w}, \mathbf{q}_1, k) = \frac{A(\mathbf{l}, \mathbf{w}, \mathbf{q}_1, k)}{S_x S_y} \quad (S_x, S_y \rightarrow \infty) \quad (3.23)$$

where  $A$  is called a "characteristic area" or "correlation area". It is a proportional constant which also equals to the integration of the correlation function ( $a$ ) (Vanmarcke 1983):

$$A(\mathbf{l}, \mathbf{w}, \mathbf{q}_1, k) = \int_{-\infty}^{+\infty} \int_{-\infty}^{+\infty} \mathbf{a}(x, y) dx dy = \int_0^{r_{\max}} 2pr \cdot \mathbf{a}(\mathbf{l}, \mathbf{w}, \mathbf{q}_1, k, r) dr \quad (3.24)$$

The validity of the asymptotic expression for the variance function (**Equation 3.23**) is subject to certain conditions on the "moments" of the correlation function. Consider **Equation 3.21**, when  $S_x$  and  $S_y$  tend toward infinity, the probability density function has only one term left which is equal to  $\frac{2pr}{S_x S_y}$ , provided the correlation function ( $a$ ) decays sufficiently rapidly.

In the case of perfectly oriented situation, the characteristic area is given by:

$$A(\mathbf{l}, \mathbf{w}, 0, 0) = \int_0^l 2pr \cdot (1 - \frac{r}{l}) dr = \frac{1}{3} pl^2 \cong l^2 \quad (3.25)$$

For completely randomized flake orientation, the characteristic area is evaluated by:

$$A(\mathbf{l}, \mathbf{w}, \frac{\mathbf{p}}{2}, 0) = \int_0^{\sqrt{l^2 + w^2}} 2\mathbf{pr} \cdot \mathbf{a}(\mathbf{l}, \mathbf{w}, \frac{\mathbf{p}}{2}, 0, r) dr = \mathbf{l}\mathbf{w} \quad (3.26)$$

which is equal to the area of a flake.

### 3.2.7. Degree of orientation

A conventional definition of percent alignment (**Equation 3.27**) was introduced by Geimer (1976), which measures the mean angle deviation from  $45^\circ$  to the geometric axes of the sample.

$$Align\% = \frac{45 - \mathbf{q}}{45} \times 100 \quad (3.27)$$

where  $\mathbf{q} = \frac{1}{n} \sum_{i=1}^n |\mathbf{q}_i|$

$\mathbf{q}_i = i^{\text{th}}$  measured angle, and

$n =$  number of measurements.

Angles are measured over the range of  $-90^\circ$  to  $+90^\circ$  with the  $0^\circ$  being the assumed mean angle. This definition can be used to define flake alignment in experimental mat where flake angles can be established. For a real board, it is more difficult to peel off the flakes layer by layer to measure the angles. Alternately, non-destructive testing method can be used to extract the horizontal density distribution of a sample board and random field theory can be used to evaluate the degree of orientation as described below.

As discussed earlier, the flake alignment can be random ( $k = 0$  in the Von Mises distribution,  $q_1 = \frac{\rho}{2}$  in the uniform distribution) and perfectly aligned ( $k = \infty$  in the Von Mises distribution,  $q_1 = 0$  in the uniform distribution). It is reasonable to consider the random orientation case as zero degree of orientation, and perfectly aligned orientation case (all flakes parallel to long axis of the panel) as 100% degree of orientation. From **Figures 3.3** and 3.4, it is easily seen that all the correlation coefficients lie within these two curves, random and oriented. Therefore, the area between any particular curve and the curve for the random case is indirectly related to the degree of flake orientation. This provided a base to define the degree of orientation of flake, *Orient* (%). The integration of correlation function (**a**) is actually the characteristic area *A* for any given range of angles in the uniform distribution and any value of  $k$  in the Von Mises distribution.

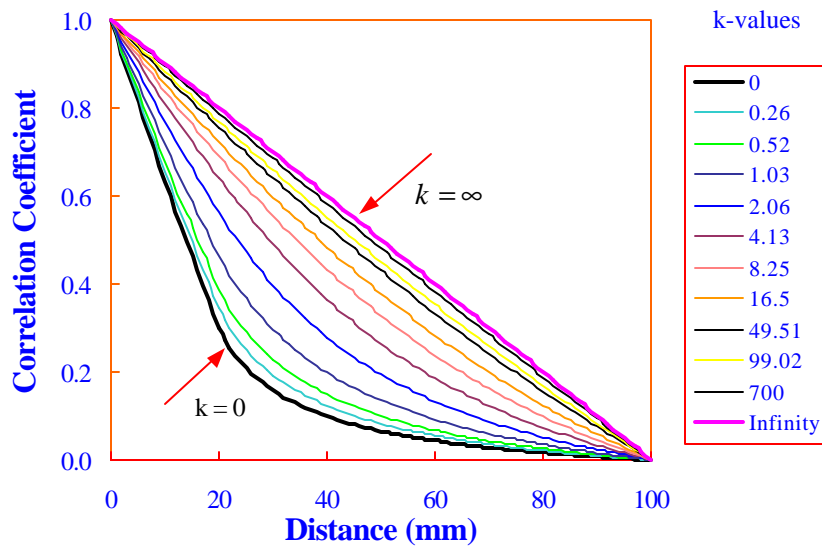


**Figure 3.3** Correlation coefficients for different values of concentration parameter  $k$  in Von Mises distribution (Flake length 100mm and width 20mm).

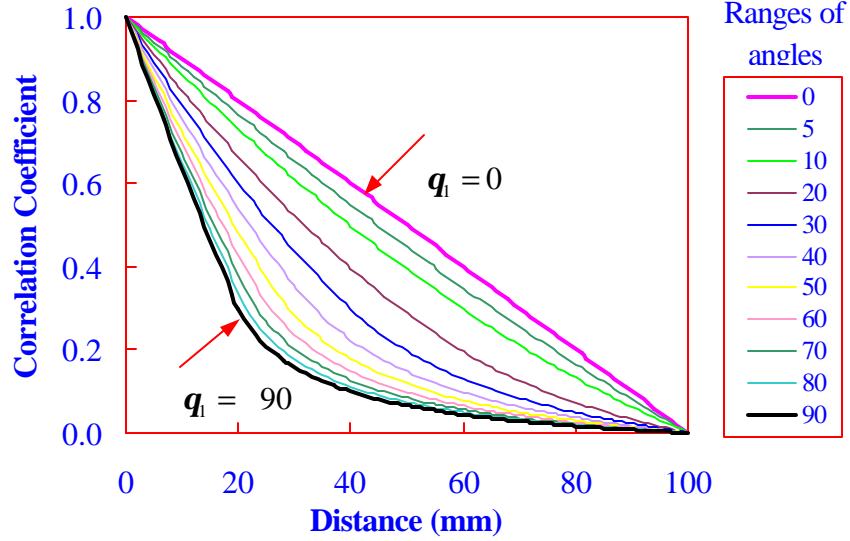


**Figure 3.4** Correlation coefficients for different ranges of angles  $q_1$  (angles represent  $\pm$ ) in uniform distribution (Flake length 100mm and width 20mm).

When  $k \neq 0$ , the flake orientation follows the Von Mises distribution with the lower bound of the random case at  $k = 0$ . When  $k = 0$ , the flake orientation is uniformly distributed within the range of  $-q_1$  to  $+q_1$  with the lower bound of the random case at  $q_1 = \frac{\pi}{2}$ . By applying the results from **Equations** 3.25 and 3.26, the degree of orientation (*Orient*) can be obtained:

$$\left\{ \begin{array}{l} \text{Orient}(k) = \sqrt{\frac{A(\mathbf{l}, \mathbf{w}, \frac{\pi}{2}, k) - A(\mathbf{l}, \mathbf{w}, \frac{\pi}{2}, 0)}{A(\mathbf{l}, \mathbf{w}, \frac{\pi}{2}, \infty) - A(\mathbf{l}, \mathbf{w}, \frac{\pi}{2}, 0)}} \times 100 = \sqrt{\frac{A(\mathbf{l}, \mathbf{w}, \frac{\pi}{2}, k) - \mathbf{l}\mathbf{w}}{\frac{1}{3}\mathbf{p}\mathbf{l}^2 - \mathbf{l}\mathbf{w}}} \times 100 \\ \text{Orient}(q_1) = \sqrt{\frac{A(\mathbf{l}, \mathbf{w}, q_1, 0) - A(\mathbf{l}, \mathbf{w}, \frac{\pi}{2}, 0)}{A(\mathbf{l}, \mathbf{w}, 0, 0) - A(\mathbf{l}, \mathbf{w}, \frac{\pi}{2}, 0)}} \times 100 = \sqrt{\frac{A(\mathbf{l}, \mathbf{w}, q_1, 0) - \mathbf{l}\mathbf{w}}{\frac{1}{3}\mathbf{p}\mathbf{l}^2 - \mathbf{l}\mathbf{w}}} \times 100 \end{array} \right. \quad (3.28)$$

Here, the square root is applied to make it compatible to the percent alignment because the percent alignment is a linear transformation of the mean angles.

In the case of the mean angle other than zero ( $\mathbf{q}_0 \neq 0$  in **Equation 3.2**), the Cartesian coordinate can always be rotated at angle  $\mathbf{q}_0$  in counterclockwise direction. Thus the above derivations for correlation coefficients, variance functions and characteristics areas are all valid for any mean angles. In the case of mapping the degree of orientation with respect to a principal direction either  $x$  or  $y$  direction, the following equations may be used.

$$\begin{aligned} \text{Orient}_x(\mathbf{q}_0, k) &= \text{Orient}(k) \cdot \left(1 - \frac{2|\mathbf{q}_0|}{\mathbf{p}}\right) \\ \text{Orient}_y(\mathbf{q}_0, k) &= 100 - \text{Orient}_x(\mathbf{q}_0, k) \end{aligned} \quad (3.29)$$

By using this mapping technique, if  $\mathbf{q}_0 = 0$ , nothing changed. But if  $\mathbf{q}_0 = \frac{\mathbf{p}}{2}$ , the degree of orientation in the  $x$  direction is zero. Similar mapping can be applied to the uniform distribution in terms of  $\mathbf{q}_0$  and  $\mathbf{q}_1$ .

### 3.3. Evaluation of Density Image Autocorrelation

A two dimensional autocorrelation function (ACF), variance function and degree of orientation for a commercial panel can be readily evaluated, provided that the density measurements of the panel in the horizontal plane  $D(x, y)$  can be obtained through some non-destructive testing methods. To determine the ACF of a digitized image, the autocovariance is calculated first as a function of various offsets and is given by Agterberg (1974) as:

$$C(r, s) = \frac{1}{(N_x - r)(N_y - s)} \sum_{x=0}^{N_x-r-1} \sum_{y=0}^{N_y-s-1} (D_{x,y} - \bar{D})(D_{x+r,y+s} - \bar{D}) \quad (3.30)$$

where

$N_x$  and  $N_y$  are the number of pixels of the image in the  $x$ - and  $y$ -directions,

$r$  and  $s$  are the offsets in the  $x$ - and  $y$ -directions,

$x$  and  $y$  are the pixel coordinates in the image, and

$\bar{D}$  is the average value of density in the image.

It is aware that  $C(0, 0)$ , which corresponds to zero offset, is the variance of density in the image. Therefore, the autocorrelation,  $Auto(r, s)$ , is obtained by dividing  $C(r, s)$  by the  $C(0,0)$  (Agterberg 1974, Pfleiderer, et al 1993) as:

$$Auto(r, s) = \frac{C(r, s)}{C(0,0)} \quad (3.31)$$

For zero offset,  $Auto(0,0) = 1$ , and with increasing offset,  $Auto(r, s)$  gradually decreases as pixels become more and more independent or statistically uncorrelated. However, this decrease is anisotropic if flakes of the panel are aligned (or partially oriented) along a preferred direction (**Figures** 3.6c to 3.6d). Therefore, by visualizing the 2-D distribution of ACF values, the degree of orientation can be calculated by **Equation** 3.28. Functions for evaluating the ACF, the variance and the degree of orientation of a density image have been added to the *density* module of **Winmat**<sup>®</sup> simulation program (Lu, et al 1998).

### 3.4. Results and Discussions

#### 3.4.1. Autocorrelation coefficient of density

It can be noted that the autocorrelation coefficients of density for any two points in a mat domain are bounded with the random case as the lower bound and perfectly aligned orientation as the upper bound. The autocorrelation coefficient of density of the perfectly aligned orientation can be characterized by any two points lying in a line ( $0 \leq r \leq l$ )

(**Equation 3.20**). The random case was well understood from Dodson's work (1971) (**Equation 3.19**). Increasing the concentration parameter  $k$  from 0 to infinity (in the Von Mises distribution) or decreasing the range of orientation angle  $\mathbf{q}_1$  from  $\frac{\pi}{2}$  to 0 (in the uniform distribution) moves the autocorrelation coefficient of density curve from its lower bound towards its upper bound (**Figures 3.3 and 3.4**).

Flake length and width are the two other factors influencing the shape of the autocorrelation coefficient of density curves since any two points covered by one larger flake may not be covered by a smaller flake. If flake length is much greater than the width ( $\mathbf{l} \gg \mathbf{w}$ ), the density autocorrelation coefficient is simplified to only one case (**Equation 3.16**). When the mean angle ( $\mathbf{q}_0$ ) changes from 0 to  $\frac{\pi}{2}$  at  $k = \infty$  ( $k = 700$  in our case), the zero autocorrelation coefficient is also changed from  $r = \mathbf{l}$  to  $r = \mathbf{w}$  (**Figure 3.5**). **Figures 3.6a to 3.6h** present the autocorrelation coefficients of density for four simulated mats. It is obvious that the density autocorrelation coefficient is one when  $x$  and  $y$  coordinates (the distance between any two points) are zeros, and zero when  $x$  and/or  $y$  go to very large. For the random mat (**Figures 3.6a and 3.6b**), the autocorrelation coefficients form many concentric cycles around the origin. **Figures 3.6c and 3.6d** represent the autocorrelation of a partially oriented flakeboard mat (range of angles from -45 to +45 degrees). For the perfectly aligned mat (**Figures 3.6e and 3.6f**), the autocorrelation coefficient of density is a linear function of the distance between two points along either the flake length direction or the flake width direction. This agrees well with the findings in **Figure 3.5**. **Figures 3.6g and 3.6h** are another representation of the autocorrelation of perfectly aligned flakeboard mat, whose flakes are oriented at 45 degrees.

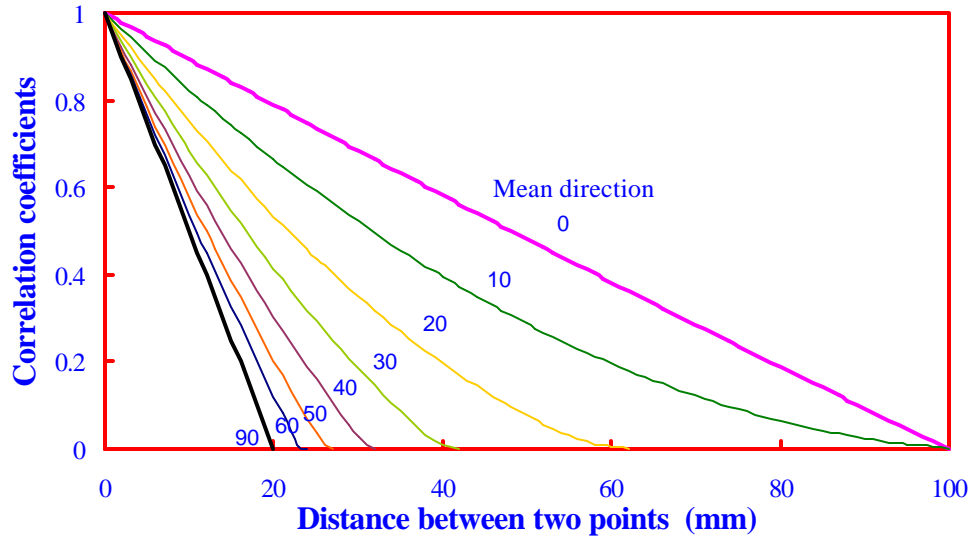


**Figure 3.5** Correlation coefficient between two points in the mat with various mean direction ( $q_0$ ) in Von Mises distribution (Flake length 100mm and width 20mm,  $k = 700$ ).

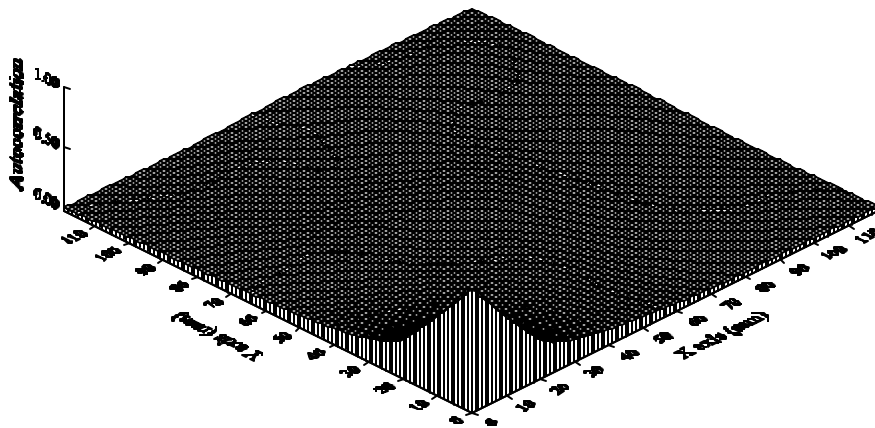


**Figure 3.6a** Correlation coefficient between two points in a mat (3D graphical representation) in completely randomized distribution of flake location and orientation (Flake length 100mm and width 20mm).

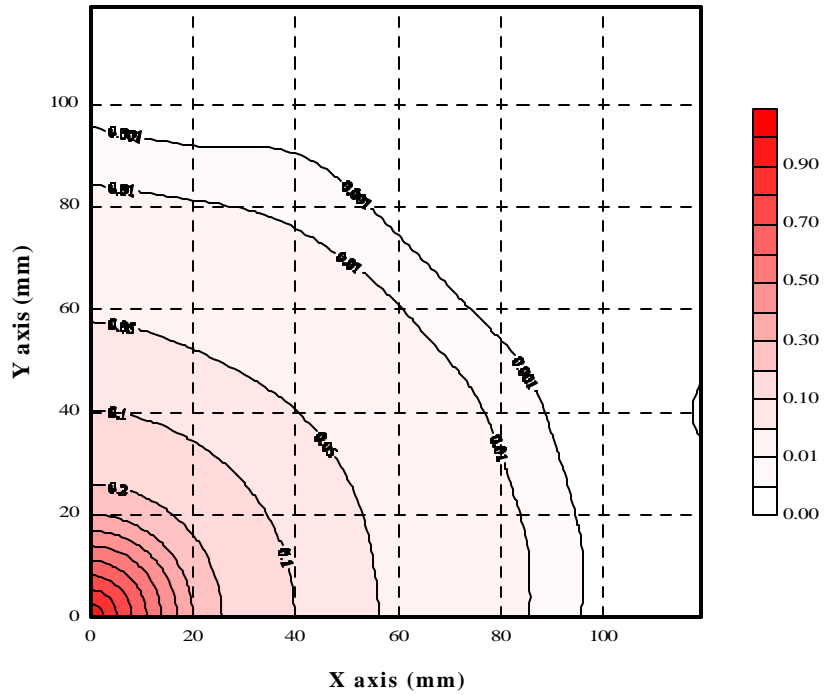


**Figure 3.6b** Correlation coefficient between two points in a mat (contour map) in completely randomized distribution of flake location and orientation (Flake length 100mm and width 20mm).

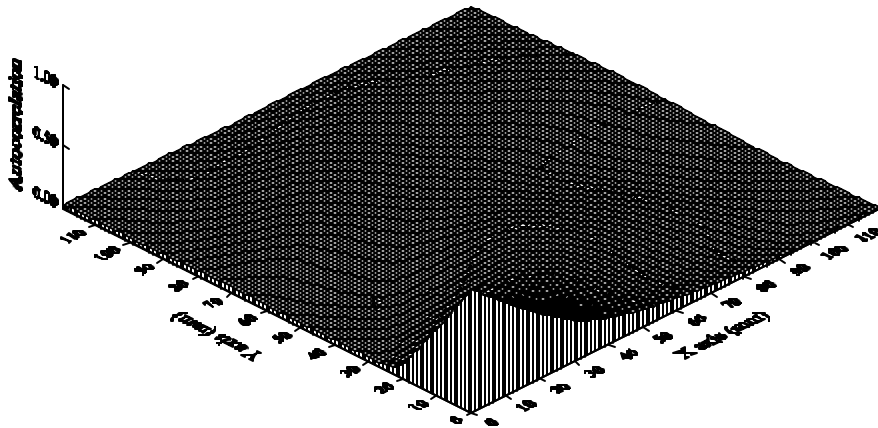


**Figure 3.6c** Correlation coefficient between two points in a mat (3D graphical representation) with partial orientation of flakes (range of angles: -45 to +45 degrees, flake length 100mm and width 20mm).

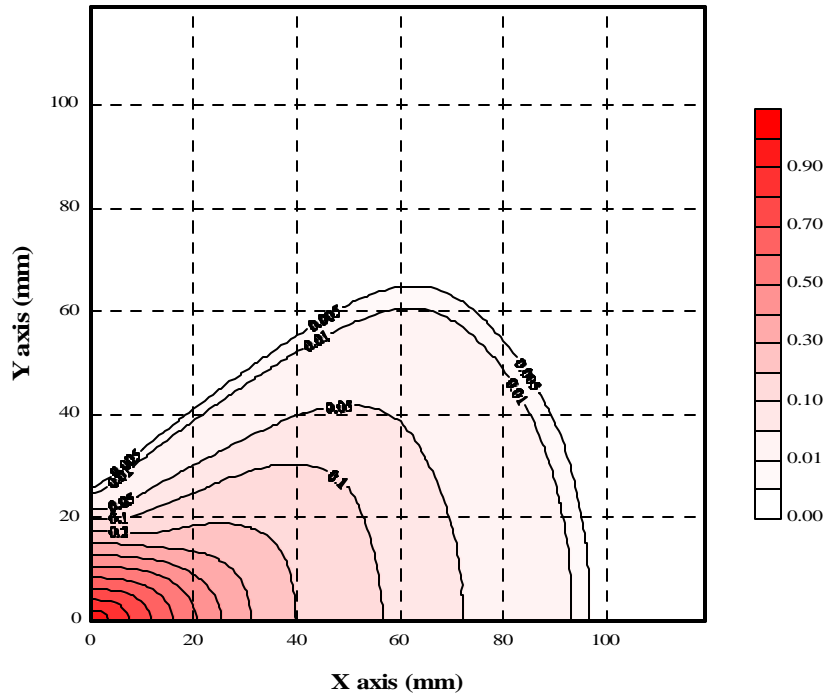


**Figure 3.6d** Correlation coefficient between two points in a mat (contour map) with partial orientation of flakes (range of angles:  $-45$  to  $+45$  degrees, flake length 100mm and width 20mm).

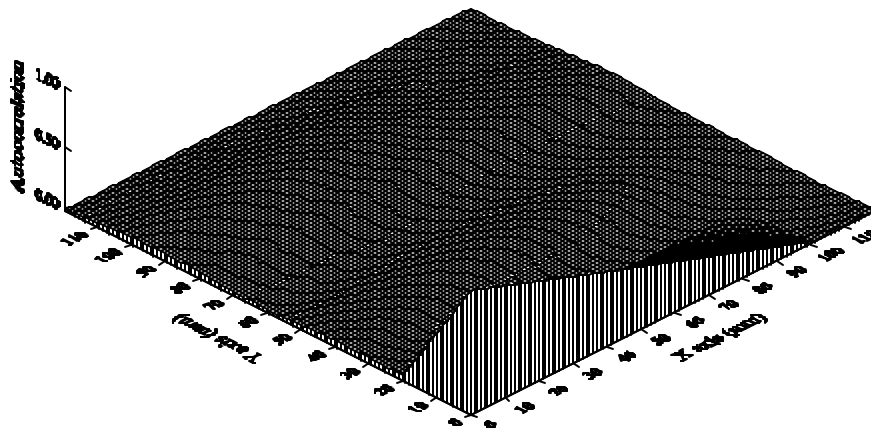


**Figure 3.6e** Correlation coefficient between two points in a mat (3D graphical representation) in perfectly aligned flake orientation ( $0^\circ$ ) and random location (Flake length 100mm and width 20mm).

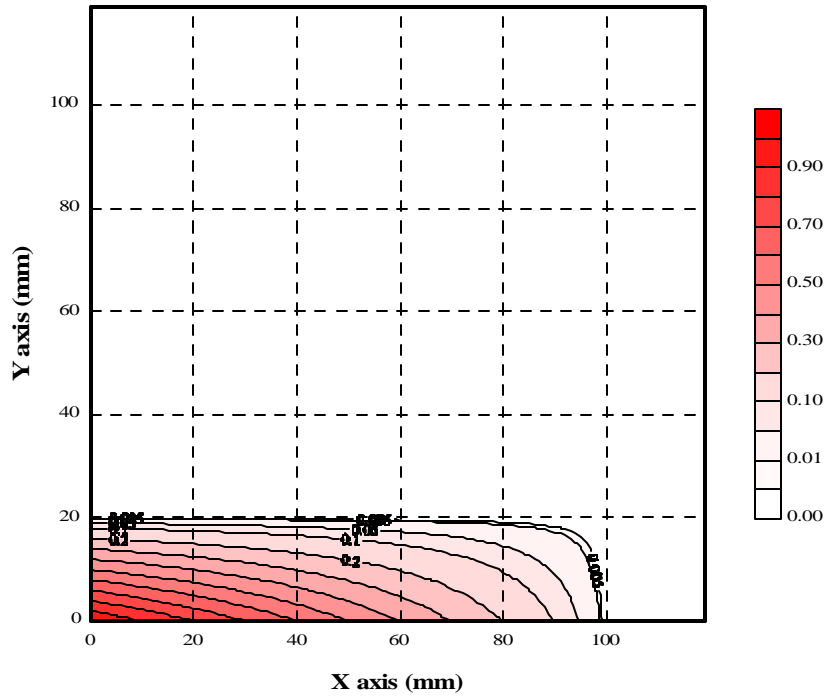


**Figure 3.6f** Correlation coefficient between two points in a mat (contour map) in perfectly aligned flake orientation ( $0^\circ$ ) and random location (Flake length 100mm and width 20mm).

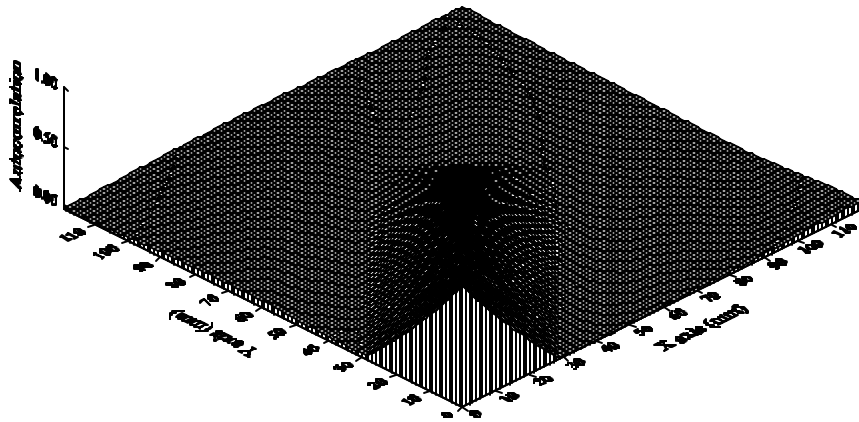


**Figure 3.6g** Correlation coefficient between two points in a mat (3D graphical representation) in perfectly aligned flake orientation ( $45^\circ$ ) and random location (Flake length 100mm and width 20mm).

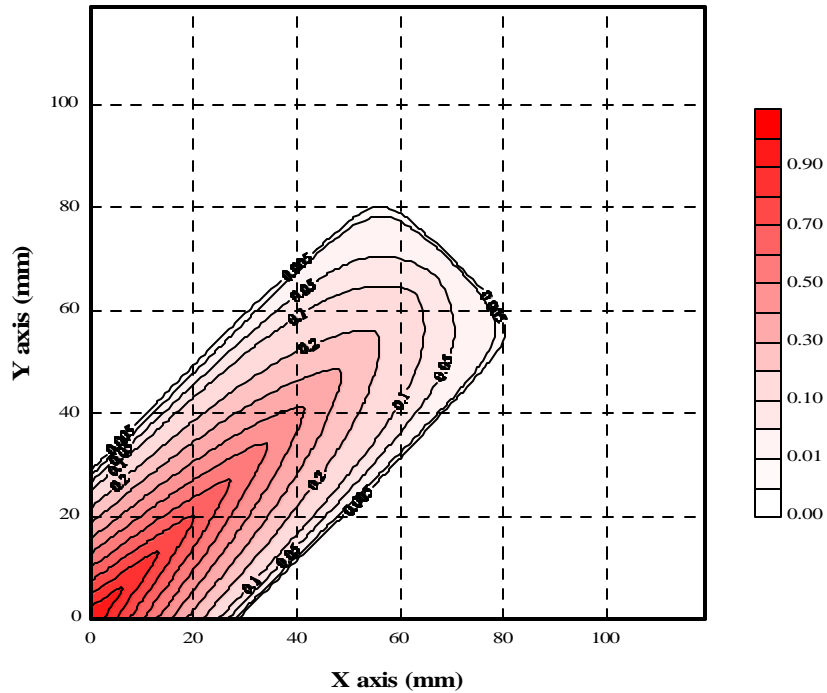


**Figure 3.6h** Correlation coefficient between two points in a mat (contour map) in perfectly aligned flake orientation ( $45^\circ$ ) and random location (Flake length 100mm and width 20mm).

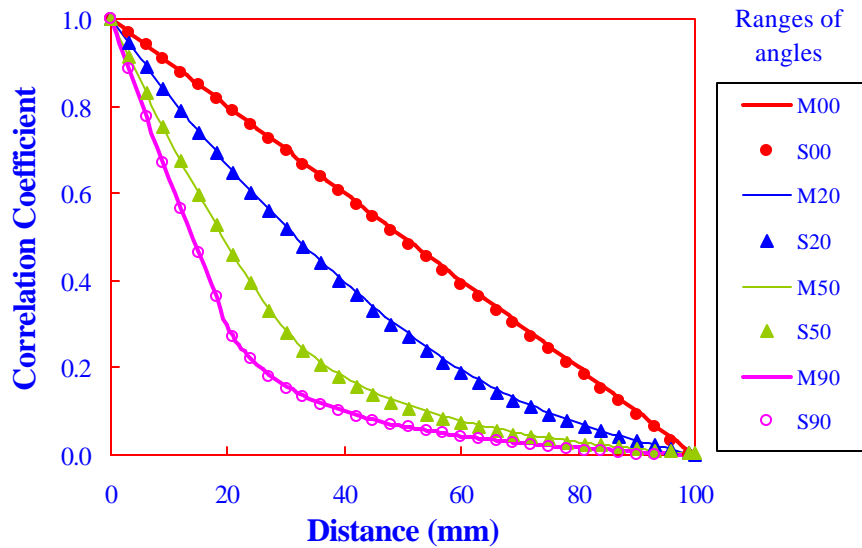


**Figure 3.7** Comparison of correlation coefficients between model prediction (lines) and computer simulation (markers) (Flake length 100mm and width 20mm).

A comparison of the autocorrelation coefficients between model prediction and computer simulation is presented in **Figure 3.7**. The simulation results agree well with the theoretically predicted values. There is a slight deviation between the predicted and simulated values when the size of simulated mat is small because an infinite domain is assumed in the mathematical model.

### **3.4.2. Variance function of density**

The distributions of variance function are plotted in **Figures 3.8** and **3.9**. When the side length of square zones is less than the diagonal length of flake, the variance reduced dramatically as the side length of square zone increases. The variance reduction rates, which reflect the speed of variance reduction, shown in **Figures 3.10** and **3.11** indicated that at the relative small sampling zones, the variance reduction rate is very high (absolute value). It becomes zero when the sampling zone size approaches infinite. It can be noted that the variance reduction rate is relatively constant at a certain level for perfectly aligned orientation at the side length of square zones less than flake length.

The variance function at the concentration parameter  $k = 700$  agrees well with the parallel case in the uniform distribution (**Figure 3.12**). Therefore, the  $k = 700$  is sufficiently large to represent the perfectly aligned situation characterized by the Von Mises distribution. The model predicted and computer simulated variance functions agree perfectly as well (**Figure 3.13**).

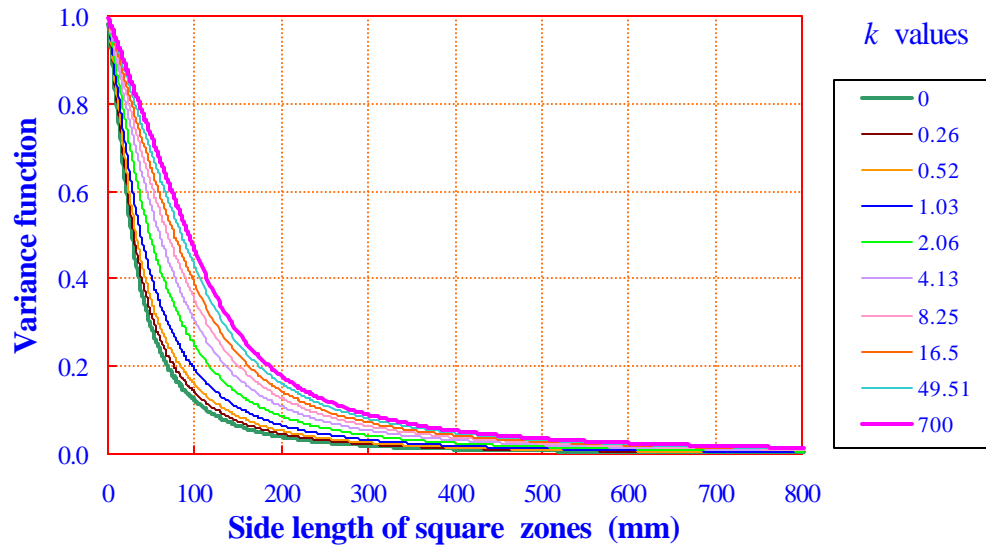


**Figure 3.8** The variance reduction with respect to different  $k$  values in Von Mises distribution and different side length of square zones (Flake length 100mm and width 20mm).

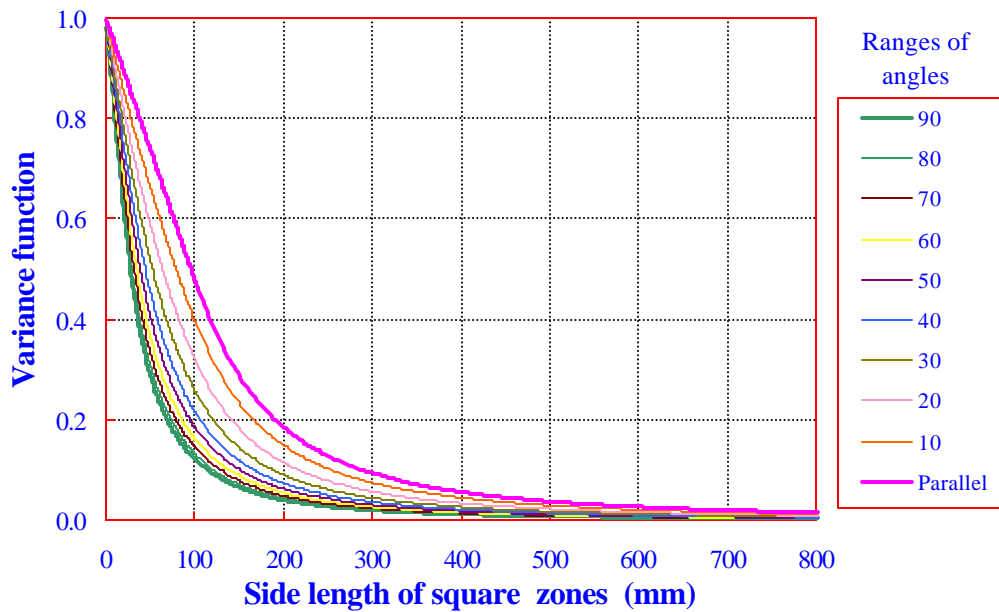


**Figure 3.9** The variance reduction with respect to different ranges of angles (angles represent  $\pm$ ) in uniform distribution and different side length of square zones (Flake length 100mm and width 20mm).

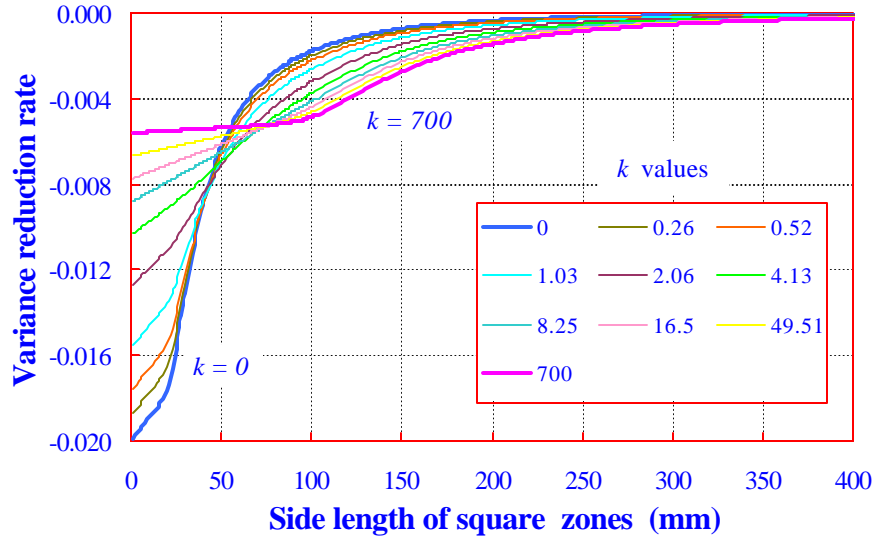


**Figure 3.10** The variance reduction rate with respect to  $k$  values in Von Mises distribution (Flake length 100mm and width 20mm).

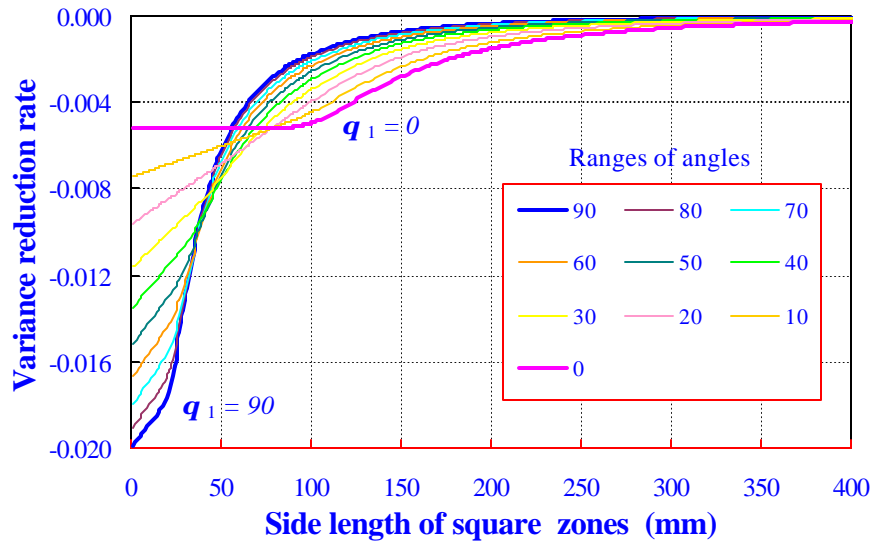


**Figure 3.11** The variance reduction rate with respect to ranges of angles (angles represent  $\pm$ ) in uniform distribution (Flake length 100mm and width 20mm).

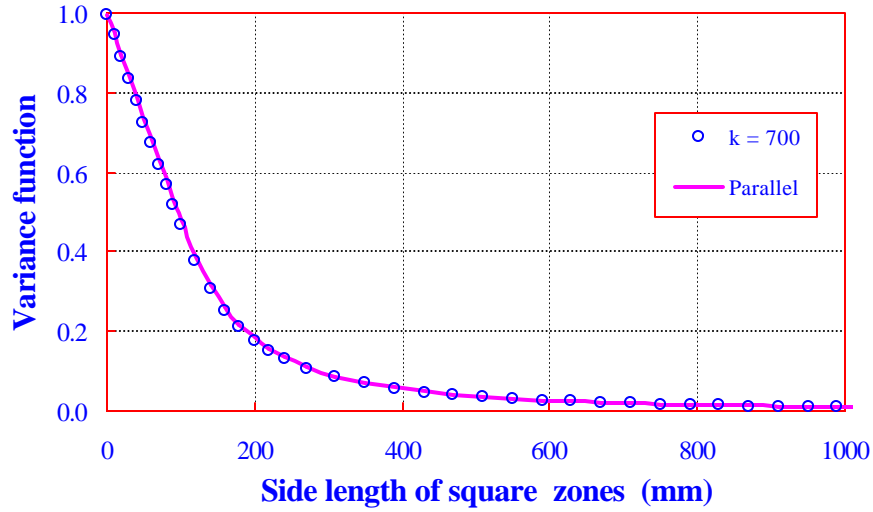


**Figure 3.12** The comparison of variance function for the perfect aligned flake by Von Mises distribution ( $k = 700$ ) and uniform distribution ( $q_1 = 0$ ) (Flake length 100mm and width 20mm).

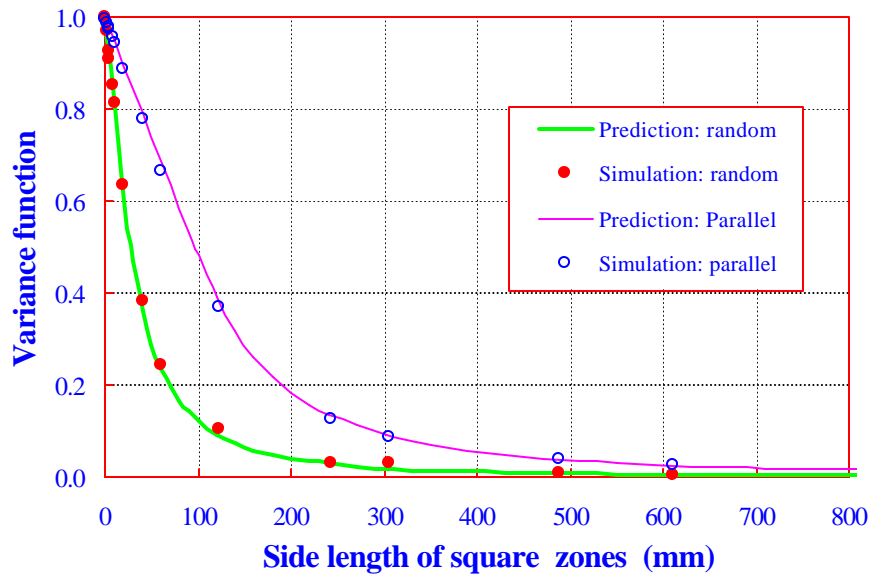


**Figure 3.13** The comparison of variance function for the randomly aligned ( $\pm 90$ ) and perfectly aligned flakes by model prediction and simulation (Flake length 100mm and width 20mm).

### 3.4.3. Characteristic area

Although it is clear that there is no variance reduction when the sampling zone reduces to a point and 100% variance reduction when the sampling zone is extremely large, the characteristic area of the correlation is not well understood. The product of variance function and the sampling zone area is constant when the sampling zone size approaches infinite. This parameter is called the characteristic area which equals to the area of a flake ( $lw$ ) in randomly oriented flakeboard mat ( $k = 0$  in the Von Mises distribution, or  $q_1 = \frac{\pi}{2}$  in the uniform distribution) (Equation 3.26). Figures 3.14 and 3.15 show that the characteristic area increases when the flakes become more oriented. It can also be noted that the maximum characteristic area is approximately equal to the square of the flake length in perfectly oriented flakeboard mat because it is independent of flake width. The characteristic area indirectly reflects the degree of variance reduction as shown in Figure 3.16. Large characteristic area indicates high average variance reduction.

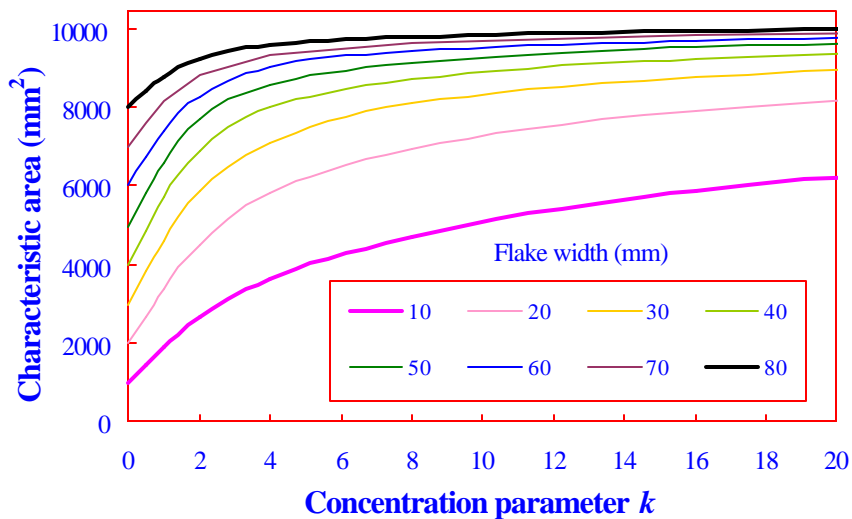


**Figure 3.14** Characteristic area in relation to the concentration parameter  $k$  in Von Mises distribution of flakes (Flake length 100mm).

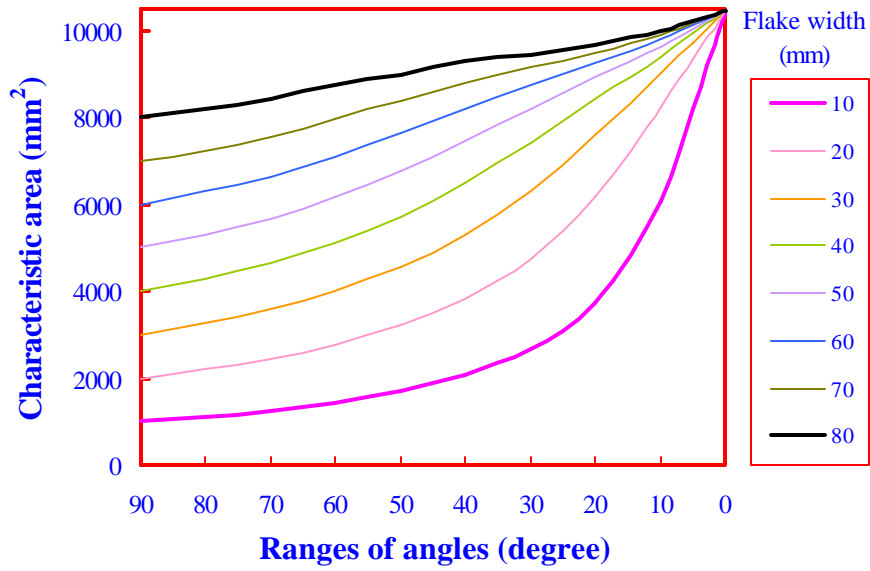


Figure 3.15 Characteristic area in relation to the ranges of angles (angles represent  $\pm$ ) in uniform distribution of flakes (Flake length 100mm).

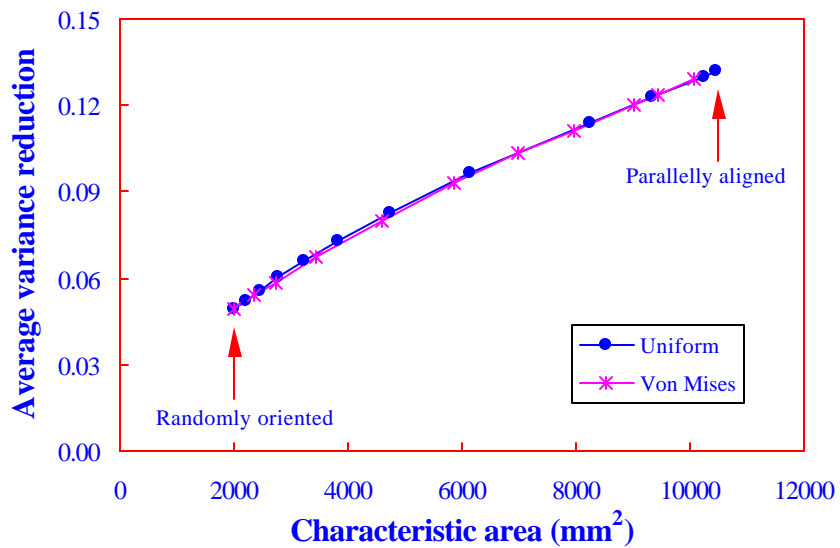


Figure 3.16 Characteristic area in relation to the average variance reduction from random orientation to perfect alignment (Flake length 100mm and width 20 mm).

#### **3.4.4. Degree of orientation**

The degree of orientation of flakes was compared with the percent alignment calculated by Geimer's formula for the mean angle at zero degree in the Von Mises distribution (**Figure 3.17**) and in the uniform distribution (**Figure 3.18**). The degree of orientation started at 0 for random orientation case and ended at 100% for the perfectly aligned arrangement in both distributions. The predicted and simulated values from characteristic areas agree well with the percent alignment values. This suggests that the degree of orientation concept can also be used to estimate the flake arrangement of commercial panels if the horizontal density distribution of the panel can be evaluated through non-destructive testing.

### **3.5. Conclusions**

The degree of orientation of flakes in structural wood-based composites, such OSB, is an important processing parameter because it determines the degree of directional strength and stiffness of the panel. A random field theory representation of the variation of horizontal density in partially oriented flakeboard mats were presented in this study.

The orientation of flakes in a mat was characterized by both the Von Mises distribution and the uniform distribution within a range of angles. Theoretical models for the correlation coefficients, variance functions, characteristic area and the degree of orientation were discussed.

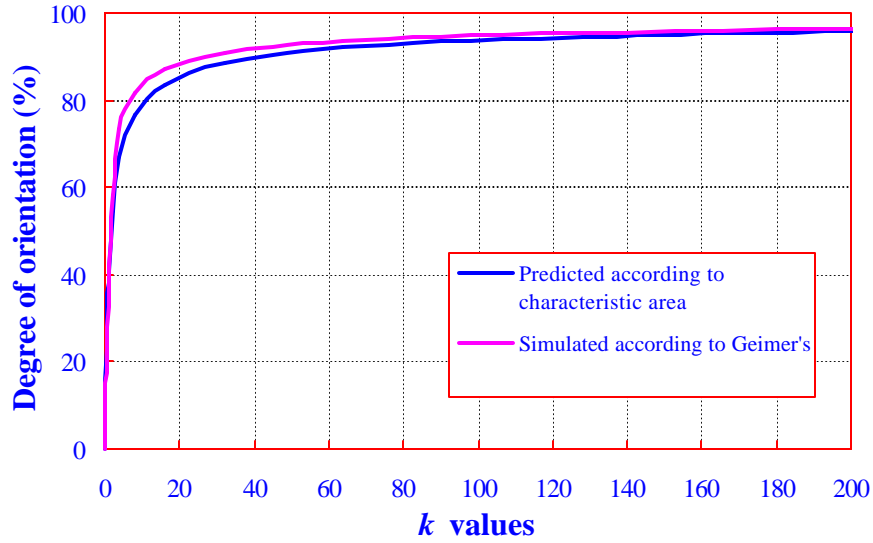


**Figure 3.17** Degree of orientation of flakes with respect to concentration parameter  $k$  in Von Mises distribution (Flake length 100mm and width 20mm).

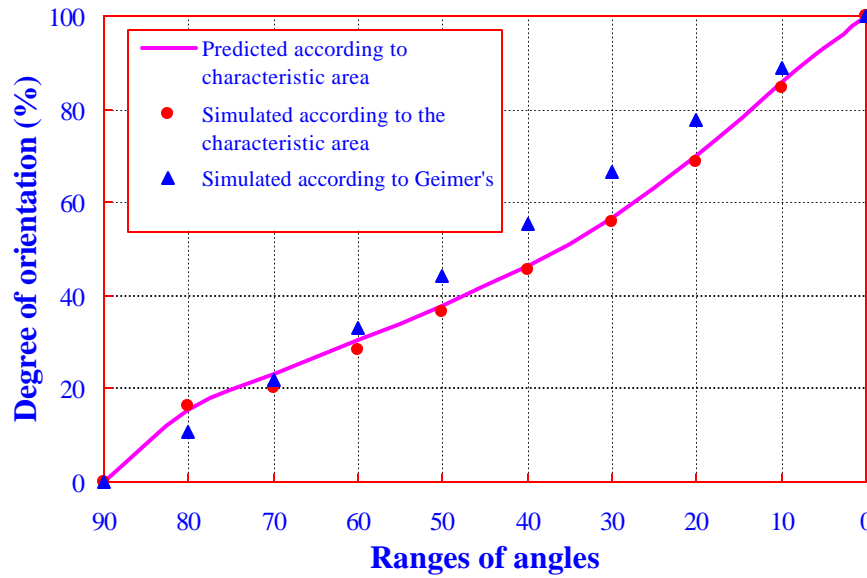


**Figure 3.18** Degree of orientation of flakes with respect to the ranges of angles (angles represent  $\pm$ ) in uniform distribution (Flake length 100mm and width 20mm).

Theoretical analysis indicated that  $k = 700$  is sufficiently large to represent the perfectly aligned orientation of flakes in Von Mises distribution. The correlation coefficients have a lower bound (random case) and an upper bound (perfectly aligned) in both distributions. Flake geometry and mean orientation angles have great influences on the correlation coefficient. The variance of density is considerably reduced as the sampling zone size increases within the length of flake and tends toward zero as the zone size goes to infinity.

The characteristic area, another measure of correlation, has the minimum and maximum values, which are expressed as the area of a flake and the approximate square of flake length, respectively. It also indirectly indicated the degree of variance reduction in partially oriented flakeboards. The degree of orientation discussed in this study is an alternate way to estimate the flake alignment of OSB products.

### **3.6. References**

Agterberg, F.P. 1974. Geomathematics: mathematical background and geo-science applications. Elsevier Scientific Publishing Co. Amsterdam. 596p

Dai, C. and P.R. Steiner. 1994. Spatial structure of wood composites in relation to processing and performance characteristics. Part 3. Modeling the formation of multi-layered random flake mats. Wood Science and Technology 28: 229-239

Dodson, C.T. J. 1971. Spatial variability and the theory of sampling in random fibrous networks. Journal of the Royal Statistical Society, Series B (Methodological), 33(1): 82-94

Geimer, R.L. 1976. Flake alignment in particleboard as affected by machine variables and

particle geometry. Research Paper 275. Madison, WI., USDA, Forest Products Lab.

Ghosh, B. 1951. Random distances within a rectangle and between two rectangles. Calcutta Math. Soc., 43:17-24

Harris, R.A. and J.A., Johnson. 1982. Characterization of flake orientation in flakeboard by the Von Mises probability distribution function. Wood and Fiber, 14(4): 254-266

Lang, E.M. and M.P., Wolcott. 1996. A model for viscoelastic consolidation of wood strand mats. Part I. Structural characterization of the mat via Monte Carlo simulation. Wood and Fiber Science, 28(1): 100-109

Lau, P.W.C. 1981. Numerical approach to predict the modulus of elasticity of oriented waferboard. Wood Science, 14: 73-85

Lu, C.; P.R. Steiner; and F. Lam. 1998. Simulation study of wood-flake composite mat structures. Forest Products Journal, 48(5): 89-93

Mardia, K.V. 1972. Statistics of Directional Data. Acad. Press, London

Pfleiderer, S; D.G.A. Ball; and R.C. Bailey. 1993. AUTO: A computer determination of the two-dimensional autocorrelation function of digital images. Computers and Geosciences, 19(6): 825-829

Shaler, S.M. 1991. Comparing two measures of flake alignment. Wood Science and Technology, 26: 53-61

Suchsland, O. and H. Xu. 1989. A simulation of the horizontal density distribution in a flakeboard. Forest Products Journal, 39(5): 29-33

*Chapter III: Random Field Representation of Horizontal Density Distribution*

Triche, M.H. and M.O. Hunt. 1993. Modeling of parallel-aligned wood strand composites. Forest Products Journal, 43(11/12): 33-44

Vanmarcke, E. 1983. Random Fields: Analysis and synthesis. The MIT Press, Cambridge, Massachusetts, London.

Xu, W. and P.R. Steiner. 1995. A statistical characterization of the horizontal density distribution in flakeboard. Wood and Fiber Science, 27(2): 160-167